AIAA JOURNAL
Vol. 38, No. 5, May 2000

Turbulence Modeling in Rotating and Curved Channels: Assessing the Spalart–Shur Correction

Michael L. Shur,* Michael K. Strelets,† and Andrey K. Travin‡
Federal Scientific Center of Applied Chemistry, St. Petersburg, 197198, Russia
and
Philippe R. Spalart§
The Boeing Company, Seattle, Washington 98124-2207

A unified approach to system-rotation and streamline-curvature effects in the framework of simple eddy-viscosity turbulence models is exercised in a range of rotating and curved channel flows. The Spalart–Allmaras (SA) one-equation turbulence model (Spalart, P. R., and Allmaras, S. R., "A One-Equation Turbulence Model for Aerodynamic Flows," AIAA Paper 92-0439, 1992) modified in this manner is shown to be quite competitive with advanced nonlinear and Reynolds-stress models and to be much more accurate than the original SA model and other eddy-viscosity models that are widely used for industrial flow computations. The new term adds about 20% to the computing cost, but does not degrade convergence.

Nomenclature

C_f, C_p	= friction and pressure coefficients
c_{b1}	= empirical constant of the Spalart–Allmaras (SA) model[10]
c_{r1}, c_{r2}, c_{r3}	= additional empirical constants of the SA rotation and/or streamline curvature (SARC) model, 1.0, 12.0, 1.0 (Ref. 7)
f_{r1}	= rotation/curvature correction function of the SARC model
Re	= Reynolds number
Ro	= Rossby number
r^*, $\tilde{r}$	= nondimensional criteria of rotation/curvature effects defined in Sec. II
$\tilde{S}$	= deformation rate in SA model[10]
S_{ij}	= components of the mean strain tensor
u_i	= components of the mean velocity vector
v^*	= friction velocity, $(\tau_w/\rho)^{1/2}$
x_i	= coordinates
ε_{jmn}	= tensor of Levi–Civita
ν_t	= eddy viscosity
$\tilde{\nu}$	= modified eddy viscosity of the SA model
ρ	= density
τ_w	= wall friction
Ω_m	= components of the system rotation rate vector
ω	= magnitude of vorticity
ω_{ij}	= components of the vorticity tensor

I. Introduction

THE surprisingly large alteration of turbulent shear flows caused by system rotation and/or streamline curvature (RC) is a well-known phenomenon that has been widely studied experimentally and numerically. On the basis of these studies, today it is widely thought that conventional linear eddy-viscosity turbulence models fail to predict this effect accurately, or even fail to predict it at all. To overcome or, at least, to alleviate that deficiency, many RC corrections for such models have been suggested (for instance, see Refs. 1–5, etc.). Though those corrections are more or less successful in the specific flows for which they were designed, they still are not universal, they treat curvature and rotation differently (in spite of their plausible common physical nature), and, in addition, often suffer from Galilean noninvariance (which is obviously undesirable).

Unlike simple eddy-viscosity models, Reynolds-stress models explicitly contain RC-production terms and, therefore, are considered as much more promising for an adequate description of curved and/or rotating turbulent flows. However, strong evidence of consistent superior accuracy for complex aerodynamic and industrial flows is not yet available.[6] This is caused, at least in part, by the high computational cost of these models: Their intensive use for real-life flows is not affordable today.

This situation motivates further attempts to develop a unified, numerically efficient, and sufficiently accurate approach for the sensitization of simple linear eddy-viscosity turbulence models to RC effects. An approach that claims to match those demands has been developed in a recent paper of Spalart and Shur.[7] It is empirical and close to that proposed by Knight and Saffman,[8] but has a somewhat different formulation and is easier to apply, especially in three-dimensions. Unlike traditional RC corrections, the Spalart and Shur[7] approach is based on a measure of the RC effects, which is Galilean invariant, fully defined in three dimensions, and unifies rotation and curvature effects. This approach was recently tested in Ref. 9 for two- and three-dimensional aerodynamic vortical flows and demonstrated rather promising capabilities.

The approach in Ref. 7 involves a combination of second derivatives of the velocity field, in contrast to first derivatives used in other approaches; this might be viewed as unattractive by computer program developers (especially with unstructured grids) and as unjustifiably complex by others using turbulence modeling. The approach also follows from a critique of invariance deficiencies and of the mainstream interpretation of curvature as an extra strain, a critique that cannot be considered as accepted by the community today.

An objective of the present study is to perform a more detailed assessment of the approach of Ref. 7 when applied to wall-bounded rotating and curved flows. More specifically, the empirical rotation function suggested in Ref. 7 will be tested for the sensitization of the Spalart–Allmaras (SA) one-equation eddy-viscosity transport model[10] to rotation and/or curvature effects (SARC model) on a set of rotating and curved channel flows that are commonly used for the validation of turbulence models' capabilities to predict the RC effect on turbulent shear flows. These flows are the fully developed (one-dimensional) turbulent flow in a plane rotating channel, which has been studied both experimentally[11,12] and by direct numerical simulation (DNS)[13,14]; the one-dimensional developed flow in a curved channel studied in experiments[15–17]; the two-dimensional flow in a channel with U-turn (experiments[18]); and the three-dimensional flow in a curved rectangular cross-section channel (experiments[19]).

Received 6 July 1998; revision received 31 October 1999; accepted for publication 8 November 1999.

*Senior Research Scientist. Member AIAA.
†Principal Scientist. Member AIAA.
‡Research Scientist.
§Boeing Technical Fellow, Boeing Commercial Airplanes, P.O. Box 3707, Aerodynamics.

The SARC predictions have been compared with the experimental and DNS data and with the corresponding predictions obtained with the original SA model,[10] with the one-equation eddy-viscosity transport model of Gulyaev et al.[20] (ν_t-92 model) (see also Ref. 21), and with the two-equation $k-\omega$ shear stress transport model of Menter[22] (M-SST model), which currently is considered as one of the most accurate two-equation turbulence models for aerodynamic and industrial flows. In addition, some of the computations are carried out with the Launder–Sharma $k-\varepsilon$ model[23] as a typical representative of the $k-\varepsilon$ models, which are most widely used in applied computational fluid dynamics codes.

II. SARC Model Formulation

As mentioned in the Introduction, the spirit of the empirical approach suggested in Ref. 7 for the sensitization of eddy-viscosity turbulence models to streamline curvature and system rotation is close to that proposed by Knight and Saffman[8] (but overlooked by later two-equation turbulence modelers). As in Ref. 8, the approach of Ref. 7 is based on tracking the direction of the principal axes of the strain tensor and, thus, is both Galilean invariant and usable in a simple model. However, it differs from Knight and Saffman[8] in many details and, in particular, avoids the troublesome step of computing and numerically differentiating the principal directions. In addition, due to an explicit formula produced in Ref. 7, the formulation is easier to apply especially in three dimensions. Knight and Saffman,[8] although applying the same invariance requirements as Ref. 7, only present applications in simple two-dimensional azimuthal flows.

When applied to the one-equation SA turbulence model[10] the ideas of Ref. 7 lead to a fairly simple modification of the original model: The only difference between the modified, or SARC, model accounting for the RC effects and the SA model is that in the former the production term in the eddy viscosity transport equation, $c_{b1}\tilde{S}\tilde{\nu}$, is multiplied by the rotation function f_{r1}:

$$f_{r1}(r^*, \tilde{r}) = (1 + c_{r1})\frac{2r^*}{1 + r^*}[1 - c_{r3}\tan^{-1}(c_{r2}\tilde{r})] - c_{r1}$$

Assuming that all of the variables and their derivatives are defined with respect to the reference frame of the calculation, which is rotating at a rate Ω, the nondimensional quantities r^* and $\tilde{r}$ are given by the following formulas (present form corrects some of the numerous typographical errors in Ref. 7):

$$r^* = S/\omega$$

$$\tilde{r} = 2\omega_{ik}S_{jk}\left(\frac{\mathrm{D}S_{ij}}{\mathrm{D}t} + (\varepsilon_{imn}S_{jn} + \varepsilon_{jmn}S_{in})\Omega_m\right)\Big/D^4$$

Here

$$S_{ij} = 0.5\left(\frac{\partial u_i}{\partial x_j} + \frac{\partial u_j}{\partial x_i}\right), \qquad \omega_{ij} = 0.5\left(\left(\frac{\partial u_i}{\partial x_j} - \frac{\partial u_j}{\partial x_i}\right) + 2\varepsilon_{mji}\Omega_m\right)$$

$$S^2 = 2S_{ij}S_{ij}, \qquad \omega^2 = 2\omega_{ij}\omega_{ij}, \qquad D^2 = 0.5(S^2 + \omega^2)$$

and $\mathrm{D}S_{ij}/\mathrm{D}t$ are the components of the Lagrangian derivative of the strain tensor. These are the second derivatives mentioned earlier. The Einstein summation convention is used. The additional constants of the model of Ref. 7 are $c_{r1} = 1.0$, $c_{r2} = 12$, and $c_{r3} = 1.0$. These values are open to refinement, while giving fair results for curved and rotating boundary layers and for free vortices.

III. Numerical Method and Sample Flows Description

For the one-dimensional flow computations we used a simple central difference scheme, whereas for the two- and three-dimensional incompressible Reynolds-averaged Navier–Stokes solution, the implicit upwind flux-differences splitting scheme of Rogers and Kwak[24] was used. The inviscid fluxes were approximated with fifth-order accuracy and the viscous fluxes with second-order accuracy. An iterative procedure for the solution of the corresponding finite difference equations is based on the line (for two-dimensions) and plane (for three-dimensions) Gauss–Seidel relaxation for the continuity and momentum equations and on the diagonally dominant alternating direction implicit approximate factorization for the turbulent variables.

The assessment of the SARC model was begun with computations of one-dimensional developed flows in rotating plane channels and in curved plane channels, which are the simplest but still quite representative tests for the evaluation of a turbulence model, especially if the saturation of the RC effects is sought. The specific rotating channel flows chosen are those commonly used for that purpose in the literature. They are the flows studied experimentally by Halleen and Johnston[11] and Johnson et al.[12] and numerically, with DNS, by Kristoffersen and Andersson[13] and by Lamballais et al.[14] In the experiments[11,12] both Reynolds and Rossby numbers based on mean flow velocity U_m, channel width D, and the rotation rate Ω were varied over a wide range ($Re = 1.15$–3.6×10^4 and $Ro = 0.0$–0.21). The DNS[13] was carried out at $Re = 5.8 \times 10^3$ with Ro values up to 0.5, and in the DNS[14] the Reynolds number was 5×10^3 whereas the Rossby number was as high as 1.5. The one-dimensional developed flows in curved channels are those of Wattendorf,[15] Eskinazi and Yeh,[16] and Hunt and Joubert.[17] These flows cover a wide range of both Reynolds numbers and channel curvature. In particular, in the experiments[15] the ratio of the internal (convex) and external (concave) channel wall radii R_1/R_2 varied from 0.8 up to 0.9, and the Reynolds numbers, based on the channel width $R_2 - R_1$ and the maximum flow velocity $U_{\max}$ were 5.295×10^4 and 9.3×10^4. In Ref. 16, the R_1/R_2 ratio was the same, whereas the Reynolds number value was as high as 1.484×10^5. Finally, Hunt and Joubert[17] studied the flow with $R_1/R_2 = 0.99$ at three values of the Reynolds number: $Re = 3 \times 10^4$, 6×10^4, and 1.3×10^5.

For the evaluation of the SARC model in the two-dimensional mode, the flow in a plane channel with a U-turn was chosen, which was studied experimentally by Monson et al.[18] This flow represents a major challenge for turbulence models because it contains both strong streamline curvature [the ratio of boundary-layer thickness to radius of curvature is of $\mathcal{O}(1)$] and massive flow separation and reattachment, that is, the features most difficult to predict with existing turbulence models. A schematic of the flow geometry is presented in Fig. 1 together with a typical computational grid (203×111) used in the computations. The flow Reynolds number based on the channel width H and mean flow velocity U_m is equal to 10^6.

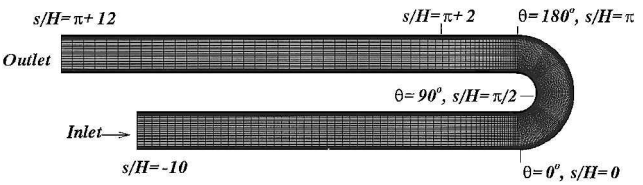

Fig. 1 Geometry of the computational domain and 203 × 111 grid used in the computations of the two-dimensional flow in a channel with U-turn[18] (every second grid line is shown).

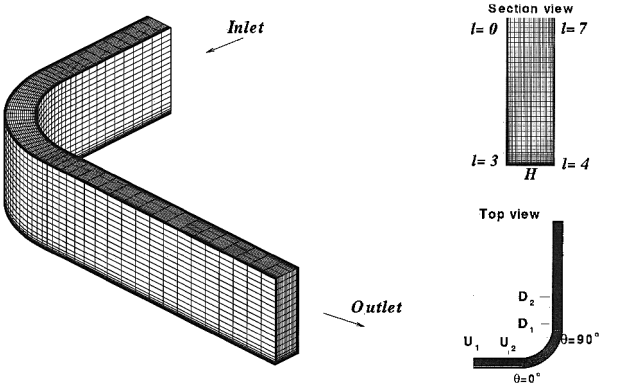

Fig. 2 Geometry of the computational domain and 121 × 81 × 61 grid used in the computations of the three-dimensional flow in a rectangular duct with 90-deg bend[19]: a) general view of the domain (half of the duct beneath the symmetry plane), b) section view, and c) top view (every second grid line is shown).

The last and the most complicated flow considered in the present study is the three-dimensional flow in a rectangular curved, with a 90-deg bend, channel studied experimentally by Kim and Patel.[19] This flow geometry and the computational grid ($121 \times 81 \times 61$) are shown in Fig. 2. This flow was suggested as a test case at the 4th and 5th International Workshops on Refined Flow Modeling[25–27] and was computed intensively with the use of a wide range of turbulence models. The duct aspect ratio D/H in the Kim and Patel[19] experiments is 6.0, the inner and outer radii of the bend, R_i and R_o, are $3H$ and $4H$, and the Reynolds number based on the freestream velocity at the reference duct section ($U_0 = 16$ m/s) and on the duct width is 2.24×10^5.

A grid-refinement study was conducted for all of the flows to guarantee that the results obtained are virtually free of numerical inaccuracies. For instance, for the channel with an U-turn (see Sec. IV.B) the difference for all of the meaningful quantities, including C_f, computed on the grids 203×111 and 301×151 was less than 1%.

IV. Results and Discussion

A. One-Dimensional Flows

Developed Flow in Plane Rotating Channels

A comparison of SARC predictions with the DNS data[13] is presented in Fig. 3. Results in Fig. 3a show that the SARC velocity profiles compare with those from the DNS fairly well: The agreement is at least not worse than that reached with the use of the Reynolds-stress model.[27–30] The correspondence between the model and DNS

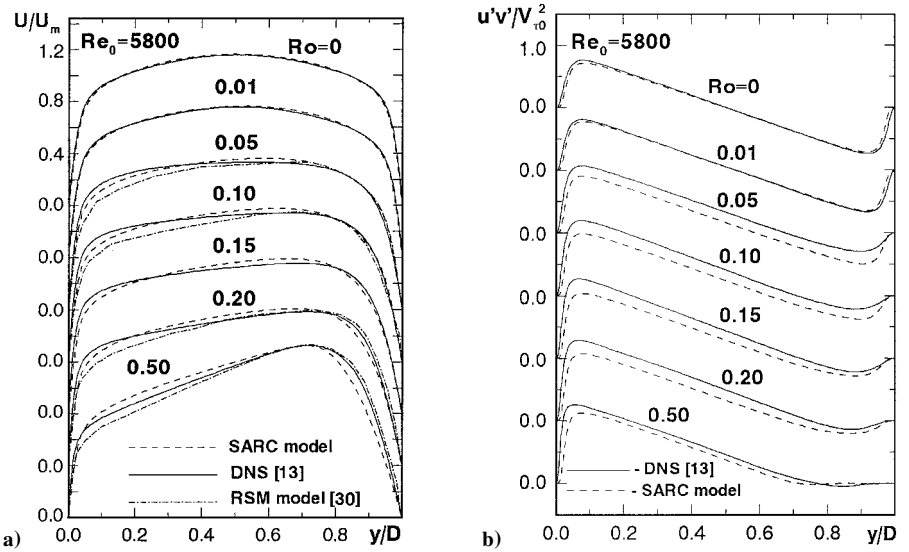

Fig. 3 Comparison of the SARC model predictions with DNS data[13] on the a) velocity and b) Reynolds stress profiles for the one-dimensional flow in a rotating plane channel.

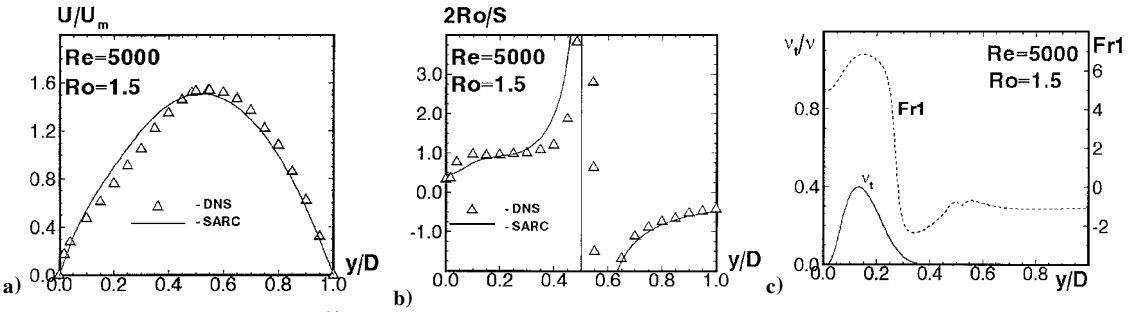

Fig. 4 SARC model predictions and DNS data[14] on the one-dimensional flow in a rotating plane channel: a) velocity profiles, b) ($2Ro/S$) profiles, and c) f_{r1} function and SARC eddy-viscosity profiles.

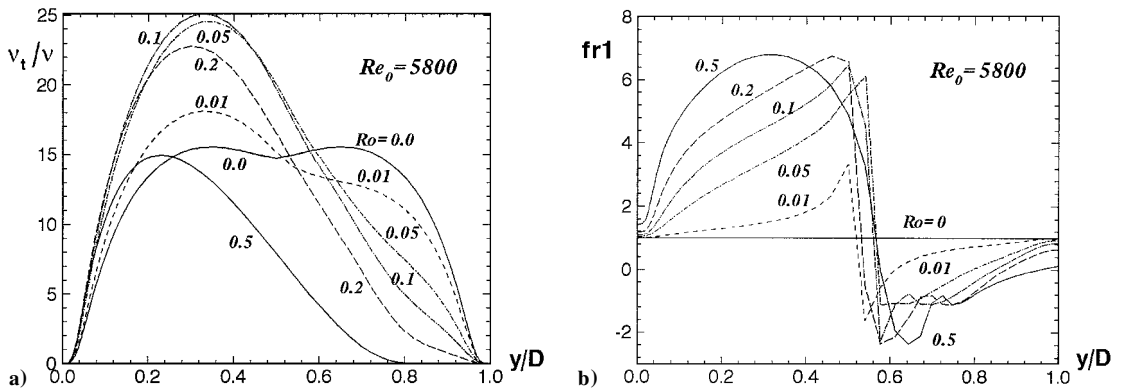

Fig. 5 Effect of Rossby number on the SARC relative eddy viscosity ν_t/ν and f_{r1}-function profiles for the one-dimensional flow in a rotating plane channel.

data on the Reynolds stress profiles (Fig. 3b), though is not as good as that for the velocity, is still quite acceptable. The same is true with regard to the DNS data[14] on the rotating channel flow with an extremely intensive rotation ($Ro = 1.5$), which is seen in Fig. 4, where the model and DNS[14] velocity profiles (Fig. 4a) and y distributions of the parameter $2Ro/S$ (Fig. 4b) are plotted.

To show the mechanism of the positive effect of the RC correction,[7] the rotation term f_{r1} distributions and the corresponding eddy-viscosity profiles are plotted in Fig. 5 at different Rossby numbers.

The quality of the SARC model prediction of the rotation effect on the wall friction is illustrated in Fig. 6, where the computed and experimental/DNS values of the ratio of the friction velocities for the rotating and stationary channels are plotted as a function of the Rossby number at the fixed (that for the stationary channel) value of the pressure gradient at three different Reynolds number values: $Re = 5.8 \times 10^3$, 1.15×10^4, and 3.5×10^4. The SARC friction at low and moderate Rossby numbers ($Ro < 0.1$) can be considered to be quite good. At the higher Rossby numbers, the model does not predict the steep drop of the skin friction at the suction wall that is observed in the experiments at low Reynolds number ($Re = 1.15 \times 10^4$, black triangles) and is caused by the flow relaminarization. Nevertheless, the current f_{r1} function provides the initial slope and some measure of saturation for Rossby number in excess of about 0.25.

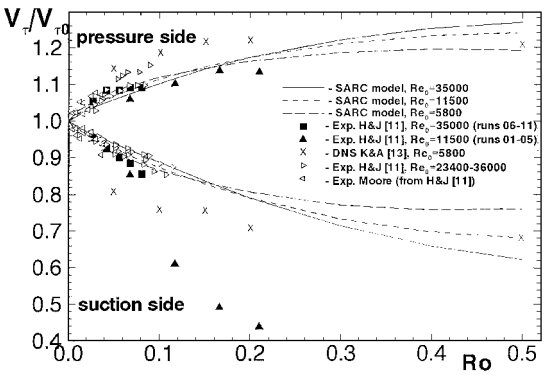

Fig. 6 Comparison of the SARC skin friction at the pressure and suction walls of the rotating plane channel with the experimental data[11,12] and DNS data[13] [$V_{\tau 0}$ is the friction velocity at $Ro = 0$, no rotation].

Developed Flow in Curved Channels

Figure 7 shows the SARC superiority over other eddy-viscosity models from the standpoint of its capability to predict the curvature effect on the friction velocity at the convex (inner) and concave (outer) walls of a slightly curved channel[17] ($R_1/R_2 = 0.99$).

In particular, according to the experiment,[17] the friction at the concave wall is tangibly (up to 20% at high Reynolds number) higher than that at the convex one. As should be expected, neither the standard SA and ν_t-92 models nor the M-SST models are capable of predicting this effect correctly: Instead, they give very close friction velocity values at both walls. The ν_t-92 model underpredicts even the lowest (convex wall) experimental friction (Fig. 7a), the M-SST model, on the contrary, gets closer to the concave wall (Fig. 7b), and the SA friction is right in the middle between the experimental data for the convex and concave walls (Fig. 7c). Introducing the f_{r1}-term (SARC model) changes the picture quite drastically: Now, the computed friction velocities at the convex and concave walls of the channel differ from each other quite tangibly and are much closer to the corresponding experimental data (see Fig. 7d). Figures 6b and 7d suggest that the best compromise would be a slightly stronger RC effect, probably obtained by increasing c_{r3} by about 20%.

Figure 8a shows the eddy-viscosity profiles computed with the different models. Note that with the SA, ν_t-92, and M-SST models they are virtually symmetric. The models do not capture the effect of the curvature on turbulence, as has been reported many times in the literature. With the SARC model, the eddy viscosity decreases near the convex wall and, on the contrary, increases near the concave wall, providing corresponding changes of the skin friction. The way that the f_{r1} term affects the eddy viscosity is clear from Fig. 8b, where f_{r1} profiles are plotted at different Reynolds numbers (curiously, they are virtually insensitive to the Reynolds number variation).

Figure 9 gives an idea of the capabilities of the SARC model for predicting the velocity profiles measured in the experiments.[15,16] In all of the cases, that is, at different Reynolds numbers (from $Re = 5.295 \times 10^4$ in the Wattendorf experiments[15] up to $Re = 1.484 \times 10^5$ in the Eskinazi and Yeh experiments[16]) and with the R_1/R_2 ratio as low as 0.8, the SARC model captures the shape of

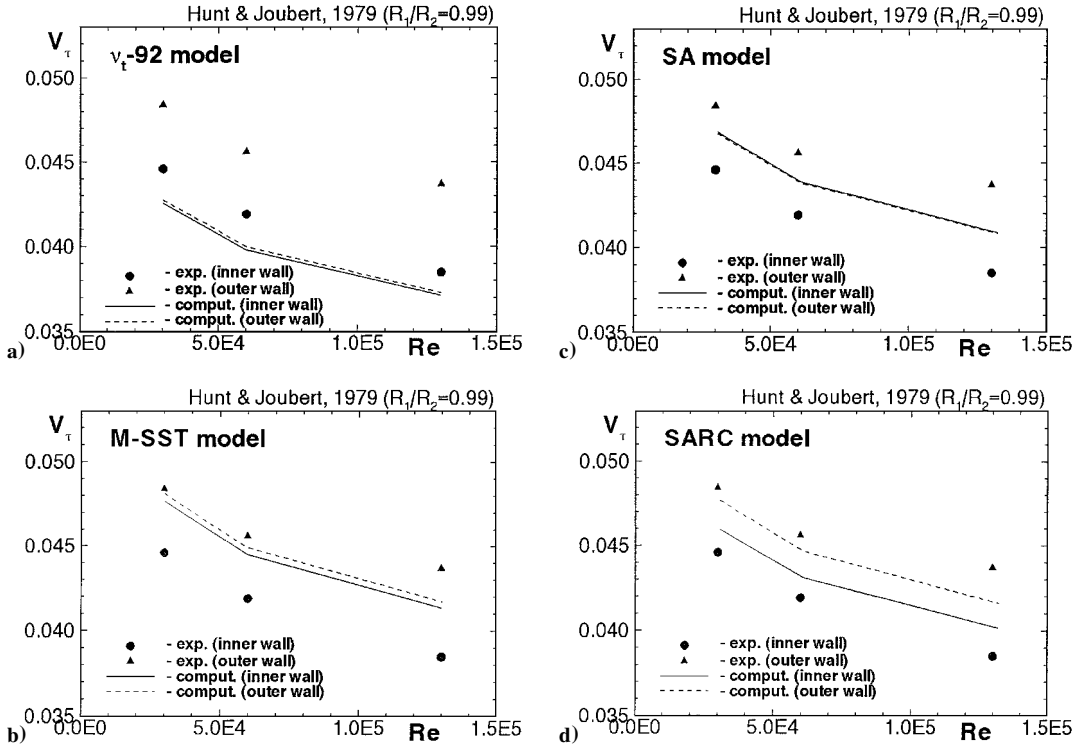

Fig. 7 Comparison of the friction velocity at the inner and outer walls predicted by different turbulence models with the experimental data[17] on the developed flow in a curved channel.

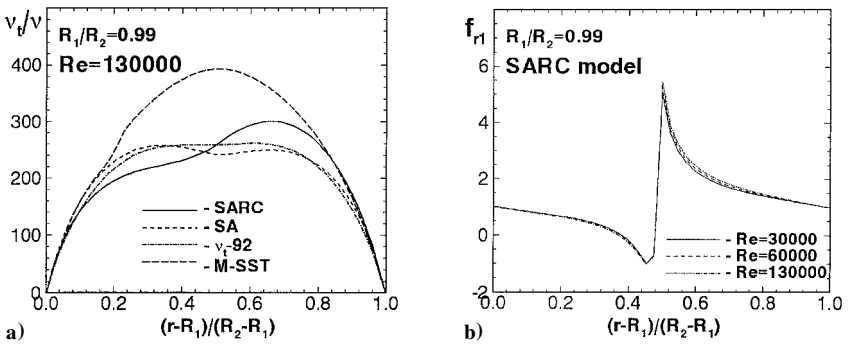

Fig. 8 Eddy viscosity for the developed flow in a slightly curved channel a) computed with different turbulence models and b) f_{r1}-function.

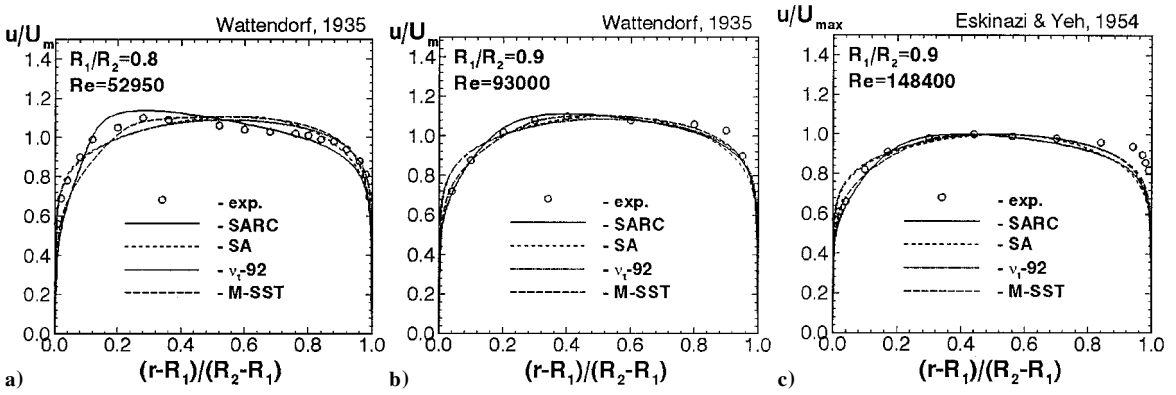

Fig. 9 Comparison of the velocity profiles predicted by different turbulence models with the experimental data.[15,16]

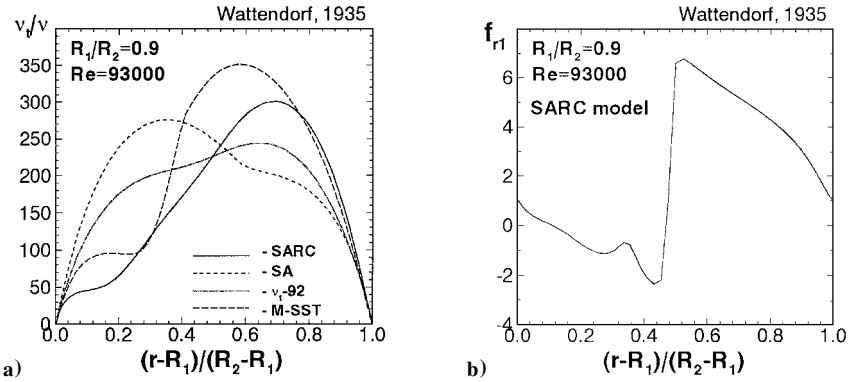

Fig. 10 Eddy viscosity for the developed flow in a strongly curved channel computed with different a) turbulence models and b) f_{r1}-functions.

the velocity profiles tangibly better than the other models; the deformation of the profiles due to wall curvature is qualitatively correct and quantitatively acceptable. An exception is the flow regime with the highest of the Reynolds numbers considered here (Fig. 9c): The SARC prediction fails to capture the shape of the velocity profile in the vicinity of the concave wall. The mechanism of the f_{r1}-term action in the SA model improvement is clear from Fig. 10, where the typical eddy viscosity and f_{r1} profiles are plotted. Note the very large excursions of f_{r1} from its passive value of 1; In some regions, the production of eddy viscosity is negative.

Thus, in general, the results presented in this section are evidence that as applied to the one-dimensional rotating and curved channel flows, the SARC model, while leaving room for improvement, provides quite acceptable predictions of the major flow characteristics.

B. Two-Dimensional Flow in a Duct with U-Turn[18]

Along with the original SA, SARC, ν_t-92, and M-SST models, this flow (see Fig. 1) was also computed with the use of Launder–Sharma k–ε model.[23] In all of the cases, in accordance with the experiment,[18] the flow at the duct section $s/H = -10.0$ (s is the distance measured along the channel central line) was assumed to be fully developed. The corresponding inlet boundary conditions for the velocity and turbulent flow quantities, ν_t, k, ω, and ε, were generated by computing the developed plane channel turbulent flow characteristics in the framework of the appropriate turbulence model. The major results of the present numerical study are presented in Figs. 11–13.

First, as clearly seen in Figs. 11–13, the accuracy of the SARC model predictions is significantly higher than that of the standard SA model. In particular, at the concave wall of the channel, both the skin-friction and pressure coefficients, C_f and C_p, computed using the SARC model are the best among all of the models considered during the present study (see Figs. 11a and 12a); the same is true with regard to the Reynolds-stress model used for this flow computation in Ref. 31. The ν_t-92 and SA models significantly underestimate the maximum C_f value. The Launder–Sharma model (LS), on the contrary, overshoots C_f at the concave wall all along the turn. Finally, the M-SST model predicts the maximum C_f value quite accurately, but farther downstream overestimates the friction. The pressure coefficient, according to the SA, ν_t-92, and LS models, is almost constant downstream of the duct cross section $\theta = 180$ deg ($s/H = \pi$, the end of the turn), whereas in the experiment, just as predicted with the SARC model, it drops significantly (in the region

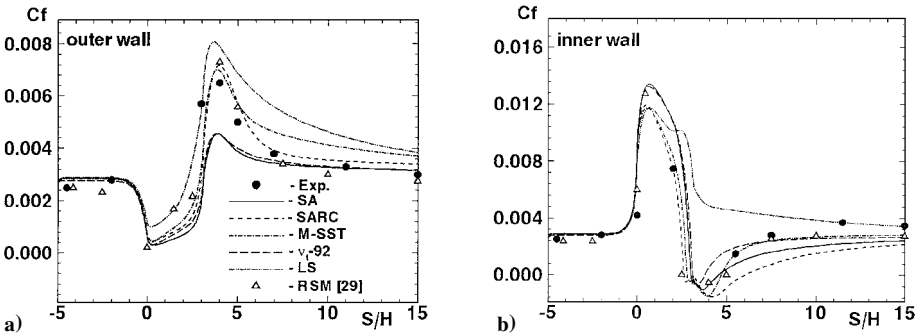

Fig. 11 Computed and measured distributions of the skin-friction coefficient of the channel with U-turn[18] along the outer and inner walls.

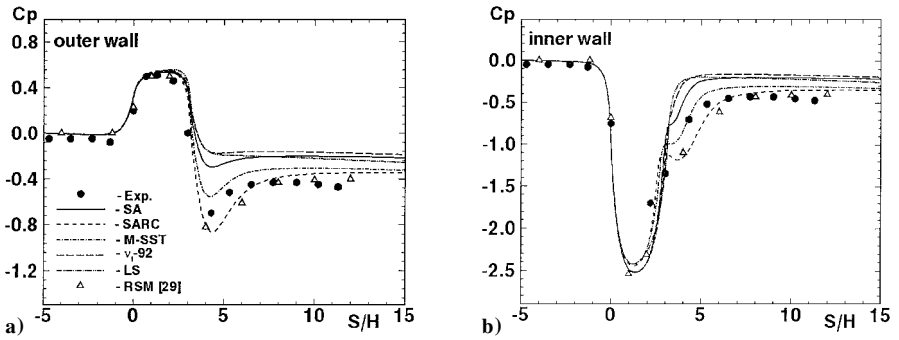

Fig. 12 Computed and measured distributions of the pressure coefficient of the channel with U-turn[18] along the outer and inner walls.

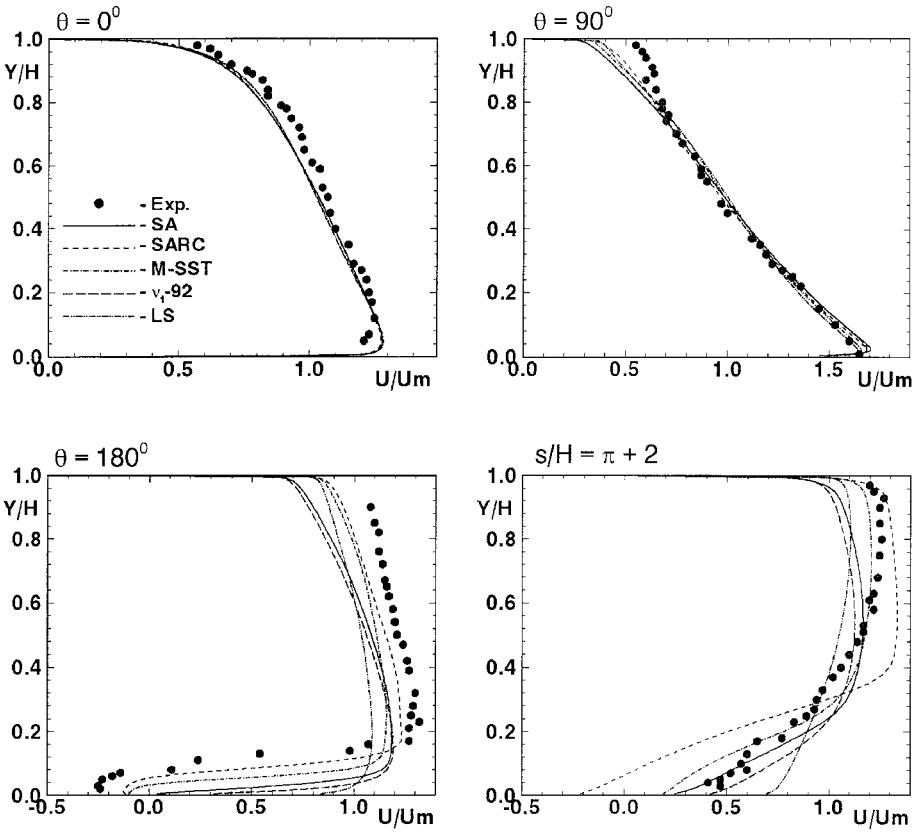

Fig. 13 Computed and measured velocity profiles at different sections of the channel with U-turn.[18]

of the flow separation from the inner wall) and only after that increases and then becomes constant. The M-SST model predicts C_p at the outer wall better than the LS, v_t-92, and SA models and is almost as good as the SARC model.

Approximately the same assessment of the relative rank of the models is found with regard to the inner wall friction and pressure distributions but only upstream of flow separation (see Figs. 11b and 12b). After separation the situation changes, at least as far as the SARC model is concerned. It tangibly overestimates the length of the recirculation zone and predicts too slow a recovery after reattachment. However, most probably, this deficiency is not associated with the f_{r1} correction and is caused by the similar deficiency of the original SA model observed earlier in plane flows with massive separation and reattachment.[21]

As to the performance of the other models at the inner wall, the LS model fails to predict separation at all (its C_f is positive everywhere), the v_t-92 model predicts too short a recirculation zone, and the M-SST model, in general, agrees with the experiment better

than the other models, though it also somewhat underestimates the rate of the flow recovery after reattachment.

All of the described trends are clearly seen not only from the skin-friction and pressure distributions, but also from the velocity profiles presented in Fig. 13; when analyzing these results note that the integrals of the experimental velocity profiles (the mass flow) have deviations from the constant value, in the 1–2% range.

A general conclusion that can be drawn on the basis of the present study of the f_{r1}-term efficiency as applied to the two-dimensional U-turn duct flow is that, although it provides some improvement compared to the original SA model, the SARC model still has deficiencies, most probably, due to the deficiencies of the original SA model rather than due to difficulties with the f_{r1} correction itself.

C. Three-Dimensional Curved Channel Flow[19]

As mentioned earlier the three-dimensional curved channel flow (Fig. 2) was intensively studied numerically in the course of the European Research Community on Flow, Turbulence and Combustion/International Association of Hydraulic Engineering and Research (ERCOFTAC/IAHR) Workshops on Refined Flow Modeling.[25–27] None of the turbulence models used by the workshop participants (starting from the conventional k–ε models and ending with the advanced algebraic and differential Reynolds-stress models) was able to predict the major flow characteristics properly. For this reason, this flow was chosen to test the claim of Ref. 7 that the f_{r1} correction is both easily handled and effective for complex three-dimensional wall-bounded turbulent flows.

The computations were performed using the SA and SARC models and, in addition, using the M-SST model, which was quite competitive with SARC for the two-dimensional U-turn duct considered in the preceding section. Note that when computing this flow, difficulties were encountered when imposing the inlet boundary conditions, due to the lack of experimental data on the mean and turbulent flow quantities in the near-wall region of the reference section of the duct (section U_1 in Fig. 2 located at $4.5H$ upstream of the bend). This was handled by first computing the three-dimensional flow at the entrance region of a straight rectangular duct having the same aspect ratio and Reynolds number as in the experiment.[19] Then the computed flow parameters in the near-wall region at the duct section with the momentum thickness Reynolds number at the center of the vertical duct wall, $Re_\theta = U_0\theta/\nu$, equal to that measured in the experiment[19] at the reference section U_1 ($Re_\theta = 1650$), were matched with the measured core flow characteristics at that section. The resulting flow parameters were used as the inlet boundary condition for subsequent computations. This approach was checked by numerical experiments using different inlet boundary conditions; due to the dominant effect of curvature, the resulting uncertainties did not affect the results of the computations in the curved section of the duct that were of interest during the present study.

The major results of the computations are presented in Figs. 14 and 15. Figure 14 illustrates the comparison between the SA, SARC, and M-SST predictions with the experimental data[19] on the streamwise evolution of the skin-friction coefficient distribution along the perimeter of the duct cross section [$l = 0$ in Fig. 14 corresponds

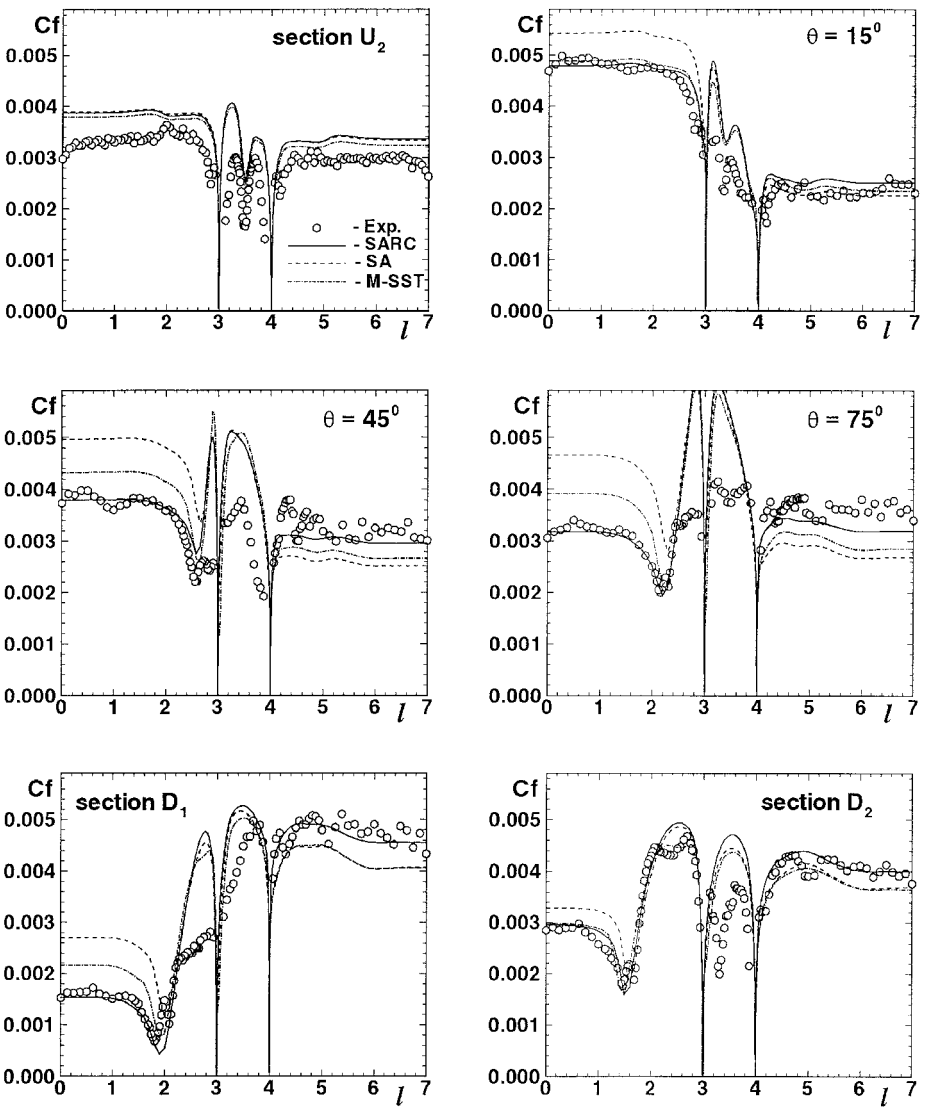

Fig. 14 Computed and measured streamwise evolution of the skin-friction distribution along the perimeter of the cross section of the rectangular duct with 90-deg bend.[19]

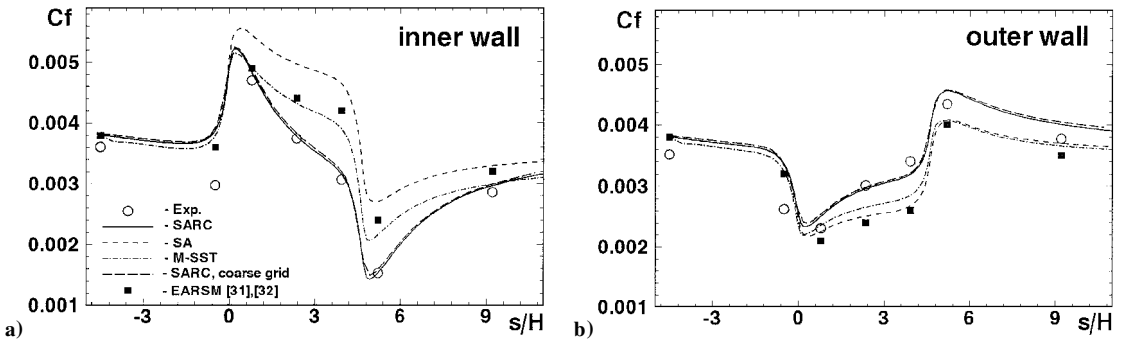

Fig. 15 Computed and measured distributions of the skin friction coefficient of the rectangular duct with 90-deg bend[19] along midspan of the inner and outer walls.

to the center of the inner (convex) vertical wall and $l = 7$ to that of the outer (concave) wall]. At the second experimental section U_2, located at $0.5H$ upstream of the beginning of the turn, all of the turbulence models yield similar results, which differ somewhat from the measured friction distribution. Apparently, this is due to the inaccuracy of the inlet boundary conditions used in our computations [note that a similar or even higher discrepancy between computed and measured $C_f(l)$ at the U_2 section was observed in all of the computations performed in the course of the workshop[27] with the use of different inlet boundary conditions and turbulence models].

At the first experimental section located in the curved part of the duct ($\theta = 15$ deg) the friction distributions become rather model dependent, at least as far as the convex wall is concerned: The original SA model significantly overshoots friction at this wall, whereas both SARC and M-SST models properly predict the friction. At the top/bottom wall, the disparity between the models is virtually negligible, all of them fail to predict the experimental friction, which is true also for the other models tested at the workshop.[27] This difficulty might be caused either by a mutual deficiency of all of the evaluated models or by some inaccuracy of the friction measurements in the experiment.[19]

At the next experimental section ($\theta = 45$ deg) the disparity between the models at the vertical walls becomes even more significant. Now only the SARC model predicts the experimental friction on both convex and concave walls. The original SA model significantly overestimates the former and underestimates the latter, and the M-SST predictions are between the SARC and SA ones. The same trends, but even more pronounced, are observed at the next experimental section, $\theta = 75$ deg. Then, in the region of the flow recovery downstream of the turn (sections D_1 and D_2 located at $0.5H$ and $4.5H$ downstream of the bend), the SARC model still predicts friction at both vertical walls quite accurately, whereas the SA and M-SST models, as earlier, overestimate C_f at the convex wall and underestimate it at the concave one, though the inaccuracy is gradually diminishing.

The superiority of the SARC model is seen more directly in Fig. 15, where the friction coefficient distributions are plotted along the midspan of the concave and convex walls (s in Fig. 15 is the distance measured along the convex wall of the duct). A similar conclusion can be drawn with regard to the relative capabilities of the SARC model and the Gatski and Speziale nonlinear model[32] in conjunction with the k–ω model of Wilcox,[33] shown to be the best one among the models tested in the course of the workshop.[27]

As to the computational aspects of the SARC model as applied to the present three-dimensional flow, its efficiency is almost the same as that of the original SA model: The CPU time needed for one global iteration with the SARC model is somewhat (~20%) larger, but the convergence rate is slightly faster. The resolution provided by the $121 \times 81 \times 61$ grid (see Fig. 2) is sufficient as confirmed by Fig. 15 in which, along with the data obtained on this fine grid, the corresponding results with a coarser grid ($61 \times 61 \times 61$) are presented.

V. Conclusions

A numerical study was performed of the capabilities of the SA one-equation turbulence model modified to account for system RC, via an extensive comparison of its predictions with experimental and DNS data in rotating and curved turbulent channel flows. This yielded the following conclusions.

1) The model describes the effect of rotation on the velocity profiles surprisingly well for a wide range of Rossby number (up to $Ro = 1.5$). Its agreement with DNS data[13,14] is better than or comparable to results found using an advanced Reynolds-stress model.[30] A comparison of SARC with measurements of velocity profiles is also fairly good. The same is true for wall friction predictions at the suction wall of the rotating channel. However, at the pressure wall, the model predicts saturation of the friction velocity at a somewhat weaker rotation rate than observed.

2) For the one-dimensional developed flows in a curved channel, the SARC model improves significantly the performance of the original SA model. Unlike the two other simple eddy-viscosity models[20,22] (see also Ref. 30) that were considered, the SARC model predicts both significant asymmetry of the velocity profiles and large differences between the skin friction at the concave and convex walls of the channel. However, it seems that the model still somewhat underestimates the effect of curvature at high Reynolds numbers and leaves room for further improvement via tuning the model constants.

3) For the two-dimensional channel flow with a U-turn[18] the SARC model performs quite satisfactorily upstream of separation. In this region, predictions of the SARC model are much better than those with the original SA model and are competitive with Reynolds-stress model predictions. Downstream of separation, the SARC model still predicts skin-friction and pressure coefficients at the outer wall of the channel quite well; however, it overestimates the length of the recirculation zone and predicts too slow a recovery after reattachment at the convex wall. The latter difficulty is caused, most probably, by a deficiency of the original SA model rather than a problem with the RC term of the SARC model. Quite unexpectedly, the M-SST model with no special RC terms provides a rather accurate flow description.

4) For the three-dimensional curved channel flow,[19] the SARC model has demonstrated significant superiority over a wide range of turbulence models starting from simple eddy-viscosity models and extending to nonlinear and Reynolds-stress models.

The results obtained during the present study substantiate the vision of Ref. 7 to provide a unified description of the effect of rotation and streamline curvature on turbulent channel flows within the framework of conventional eddy-viscosity turbulence models. Even when coupled with the simple one-equation eddy-viscosity SA model, the approach of Ref. 7 provides a significant improvement for a wide range of rotating/curved channel flows. This improvement might be enhanced by a fine tuning of the model constants. No particular numerical difficulties were encountered. The assertion that all scalar eddy-viscosity models are ineffective when treating rotation and curvature is simply incorrect. Considering that similar conclusions with regard to the approach of Ref. 7 were drawn for some vortical flows,[9] it appears that this approach is worth applying to sensitize other eddy-viscosity turbulence models to rotation and curvature. The first candidate for such a modification might be the M-SST model, which is known as one of the best models of that type. Recall that the quantities r^* and $\tilde{r}$ are quite usable with scalar models other than SA; the core of Ref. 7 is the construction of $\tilde{r}$, not

the f_{r1} function (although model developers might be interested in its limiting behavior, for small r^* and for large $|\tilde{r}|$).

Acknowledgments

This work was funded by the Boeing Operation International, Inc., and was partially supported by the Russian Basic Research Foundation (Grant 97-02-16492).

References

[1]Howard, J. H. G., Patankar, S. V., and Bordynuik, R. M., "Flow Predictions in Rotating Ducts Using Coriolis-Modified Turbulence Models," *Journal of Fluids Engineering*, Vol. 102, No. 4, 1980, pp. 456–461.

[2]Launder, B. E., Priddin, C. H., and Sharma, B. I., "The Calculation of Turbulent Boundary Layers on Spinning and Curved Surfaces," *Journal of Fluids Engineering*, Vol. 99, No. 1, 1977, pp. 231–239.

[3]Park, S. V., and Chung, M. K., "Curvature-Dependent Two-Equation Model for Prediction of Turbulent Recirculating Flows," *AIAA Journal*, Vol. 27, No. 3, 1989, pp. 340–344.

[4]Gooray, A. M., Watkins, C. B., and Aung, W., "Improvements to the k–ε Model for Calculation of Turbulent Recirculating Flow," *Proceedings of the 5th Symposium on Turbulent Shear Flows*, Cornell Univ., Ithaca, NY, 1985, pp. 18.26–18.31.

[5]Leschziner, M. A., and Rodi, W., "Calculation of Annular and Twin Parallel Jets Using Various Discretization Schemes and Turbulence-Model Variations," *Journal of Fluids Engineering*, Vol. 103, No. 2, 1981, pp. 352–360.

[6]Lien, F. S., and Leschziner, M. A., "Modeling 2D Separation from a High Lift Airfoil with a Non-Linear Eddy-Viscosity Model and Second Moment Closure," *Aeronautical Journal*, Vol. 99, No. 984, 1995, pp. 125–144.

[7]Spalart, P. R., and Shur, M. L., "On the Sensitization of Turbulence Models to Rotation and Curvature," *Aerospace Science and Technology*, Vol. 1, No. 5, 1997, pp. 297–302.

[8]Knight, D. D., and Saffman, P. C., "Turbulence Model Predictions for Flows with Significant Mean Streamline Curvature," AIAA Paper 78-258, 1978.

[9]Shur, M., Strelets, M., Travin, A., and Spalart, P. R., "Two Numerical Studies of Trailing Vortices," AIAA Paper 98-0595, Jan. 1998.

[10]Spalart, P. R., and Allmaras, S. R., "A One-Equation Turbulence Model for Aerodynamic Flows," AIAA Paper 92-0439, Jan. 1992.

[11]Halleen, R. M., and Johnston, J. P., "The Influence of Rotation on Flow in a Long Rectangular Channel—An Experimental Study," Dept. of Mechanical Engineering, Rept. MD-18, Stanford Univ., Stanford, CA, May 1967.

[12]Johnston, J. P., Halleen, R. M., and Lezius, K., "Effects of Spanwise Rotation on the Structure of Two-Dimensional Fully Developed Turbulent Channel Flow," *Journal of Fluid Mechanics*, Vol. 56, Pt. 3, Dec. 1972, pp. 533–557.

[13]Kristoffersen, R., and Andersson, H. I., "Direct Simulation of Low-Reynolds-Number Turbulent Flow in a Rotating Channel," *Journal of Fluid Mechanics*, Vol. 256, Nov. 1993, pp. 163–197.

[14]Lamballais, E., Lesieur, M., and Metais, O., "Effects of Spanwise Rotation on the Stretching in Transitional and Turbulent Channel Flow," *International Journal Heat and Fluid Flow*, Vol. 17, No. 3, 1996, pp. 324–332.

[15]Wattendorf, F. L., "Study of the Effect of Curvature on Fully Developed Turbulent Flow," *Proceedings of Royal Society, Series A: Mathematical and Physical Sciences*, Vol. 148, 1935, p. 565.

[16]Eskinazi, S., and Yeh, H., "AnInvestigation of Fully Developed Turbulent Flows in a Curved Channel," *Journal Aerospace Science*, Vol. 23, 1956, p. 23.

[17]Hunt, I. A., and Joubert, P. N., "Effects of Small Streamline Curvature on Turbulent Duct Flow," *Journal of Fluid Mechanics*, Vol. 91, Pt. 4, April 1979, pp. 633–659.

[18]Monson, D. J., Seegmiller, H. L., McConnaughey, P. K., and Chen, Y. S., "Comparison of Experiment with Calculations Using Curvature-Corrected Zero and Two Equation Turbulence Models for a Two-Dimensional U-Duct," AIAA Paper 90-1484, 1990.

[19]Kim, W. J., and Patel, V. C., "Origin and Decay of Longitudinal Vortices in Developing Flow in a Curved Rectangular Duct," *Journal of Fluids Engineering*, Vol. 116, No. 1, 1994, p. 45.

[20]Gulyaev, A. N., Kozlov, V. Y., and Secundov, A. N., "A Universal One-Equation Model for Turbulent Viscosity," *Fluid Dynamics*, Vol. 28, No. 4, 1993, pp. 485–494 (translated from Russian, Consultants Bureau, New York).

[21]Shur, M., Strelets, M., Zaikov, L., Gulyaev, A., Kozlov, V., and Secundov, A., "Comparative Numerical Testing of One- and Two-Equation Turbulence Models for Flows with Separation and Reattachment," AIAA Paper 95-0863, 1995.

[22]Menter, F. R., "Zonal Two Equation k–ω Turbulence Models for Aerodynamic Flows," AIAA Paper 93-2906, 1993.

[23]Launder, B. E., and Sharma, B. I., "Application of the Energy Dissipation Model of Turbulence to the Calculation of Flow Near a Spinning Disk," *Letters in Heat and Mass Transfer*, Vol. 1, 1974, pp. 131–138.

[24]Rogers, S. E., and Kwak, D., "An Upwind Differencing Scheme for the Time-Accurate Incompressible Navier–Stokes Equations," AIAA Paper 88-2583, 1988.

[25]Bonnin, J. C., Buchal, T., and Rodi, W., "ERCOFTAC Workshop on Data Bases and Testing of Calculation Methods for Turbulent Flows," *ERCOFTAC Bulletin*, Vol. 28, 1996, pp. 48–54.

[26]Bonnin, J. C., Buchal, T., and Rodi, W., "ERCOFTAC Workshop on Data Bases and Testing of Calculation Methods for Turbulent Flows," *ERCOFTAC Bulletin*, Vol. 28, 1996, pp. 48–54.

[27]Laurence, D., "5th ERCOFTAC Workshop on Refine Flow Modelling for Turbulent Flows," *ERCOFTAC Bulletin*, Vol. 33, 1997, pp. 10–13.

[28]Launder, B. E., Tselepidakis, D. P., and Younis, B. A., "A Second Moment Closure Study of Rotating Channel Flow," *Journal of Fluid Mechanics*, Vol. 183, Oct. 1987, pp. 63–75.

[29]Fu, S., Rung, T., and Thiele, F., "Realizability of Non-Linear Stress-Strain Relationships for Reynolds-Stress Closures," *Proceedings of 11th Symposium on Turbulent Shear Flows*, Vol. 2, INPG, Grenoble, France, 1997, pp. 13.1–13.6.

[30]Andersson, H. I., "Turbulent Shear Flows Affected by Coriolis Forces," *ERCOFTAC Bulletin*, Vol. 32, 1997, pp. 25–28.

[31]Luo, J., and Lakshminarayana, B., "Prediction of Strongly Curved Turbulent Duct Flows with Reynolds Stress Model," *AIAA Journal*, Vol. 35, No. 1, 1997, pp. 91–98.

[32]Gatski, T. B., and Speziale, C. G., "On Explicit Algebraic Stress Models for Complex Turbulent Flows," *Journal of Fluid Mechanics*, Vol. 254, Sept. 1993, pp. 59–78.

[33]Wilcox, D. C., "Reassessment of the Scale Determining Equation for Advanced Turbulence Models," *AIAA Journal*, Vol. 26, No. 11, 1988, pp. 1299–1310.

C. G. Speziale
Associate Editor